Molecular Therapy
Original Article

Retained Plasticity and Substantial Recovery of Rod-Mediated Visual Acuity at the Visual Cortex in Blind Adult Mice with Retinal Dystrophy

Koji M. Nishiguchi,[1,2] Kosuke Fujita,[3] Naoyuki Tokashiki,[2] Hiroshi Komamura,[2] Sayaka Takemoto-Kimura,[4,5] Hiroyuki Okuno,[6] Haruhiko Bito,[7] and Toru Nakazawa[1,2,3]

[1]Department of Advanced Ophthalmic Medicine, Tohoku University Graduate School of Medicine, Sendai 980-8574, Japan; [2]Department of Ophthalmology, Tohoku University Graduate School of Medicine, Sendai 980-8574, Japan; [3]Department of Retinal Disease Control, Tohoku University Graduate School of Medicine, Sendai 980-8574, Japan; [4]Department of Neuroscience I, Research Institute of Environmental Medicine, Nagoya University, Nagoya 464-8601, Japan; [5]PRESTO-Japan Science and Technology Agency, Chiyoda-ku, Tokyo, Japan; [6]Medical Innovation Center, Graduate School of Medicine, Kyoto University, Kyoto 606-8501, Japan; [7]Department of Neurochemistry, Graduate School of Medicine, University of Tokyo, Tokyo 113-0033, Japan

In patients born blind with retinal dystrophies, understanding the critical periods of cortical plasticity is important for successful visual restoration. In this study, we sought to model childhood blindness and investigate the plasticity of visual pathways. To this end, we generated double-mutant (*Pde6c*$^{cpfl1/cpfl1}$*Gnat1*$^{IRD2/IRD2}$) mice with absent rod and cone photoreceptor function, and we evaluated their response for restoring rod (*GNAT1*) function through gene therapy. Despite the limited effectiveness of gene therapy in restoring visual acuity in patients with retinal dystrophy, visual acuity was, unexpectedly, successfully restored in the mice at the level of the primary visual cortex in this study. This success in visual restoration, defined by changes in the quantified optokinetic response and pattern visually evoked potential, was achieved regardless of the age at treatment (up to 16 months). In the contralateral visual cortex, cortical plasticity, tagged with light-triggered transcription of *Arc*, was also restored after the treatment in blind mice carrying an *Arc* promoter-driven reporter gene, *dVenus*. Our results demonstrate the remarkable plasticity of visual circuits for one of the two photoreceptor mechanisms in older as well as younger mice with congenital blindness due to retinal dystrophies.

INTRODUCTION

When treating an ocular disease that affects vision from birth or early childhood, it is important to provide medical intervention during certain windows of treatment opportunity or critical periods in which the plasticity of the primary visual pathway allows for useful visual restoration. Failure to comply with this period leads to lasting visual dysfunction often at the level of the visual cortex, resulting in amblyopia that affects ~3% of adults in the developed countries.[1] Considering the vulnerability of the visual system to sensory deprivation, it is believed that older children and adults with early-onset blindness, including those with inherited retinal dystrophies,[2] exhibit a limited recovery of visual acuity even following the successful restoration of the ocular function.[3–6] Indeed, in a series of gene therapy clinical trials targeting retinal dystrophy with severe visual dysfunction from birth,[3,7,8] increased sensitivity to light was reproducibly demonstrated across different trials, indicating that the ocular treatment itself was successful and that adult neuroplasticity is present for this functional aspect of vision. However, the improvement of visual acuity, which requires more complex visual processing, was inconsistent in both children and young adults, although the vast majority of patients treated were below the age of 30.[4,9–12] Nevertheless, the youngest child treated in these studies was 4 years old, leaving open the possibility that a critical period for successful visual acuity restoration in congenital retinal dystrophies exists at an even younger age range. Indeed, studies of congenital cataract have shown that the successful improvement in visual acuity is limited to the very first few months after birth.[13–15] However, the plasticity of the visual system has never been extensively studied in the animal models of retinal dystrophies.

RESULTS

Pde6c$^{cpfl1/cpfl1}$ Gnat1$^{IRD2/IRD2}$ Mice Are Virtually Blind

To define the critical period for the restoration of visual acuity in mice with blinding congenital retinal dysfunction, we generated double-mutant *Pde6c*$^{cpfl1/cpfl1}$*Gnat1*$^{IRD2/IRD2}$ mice that were almost completely defective in both cone and rod function by crossing rod-defective *Gnat1*$^{IRD2/IRD2}$ mice[16–18] and cone-defective *Pde6c* $^{cpfl1/cpfl1}$ mice.[19] In the double mutants, we found that the rods comprising ~97% of the recoverin-positive photoreceptors degenerated minimally over the course of 9 months, whereas most PNA (peanut agglutinin)-labeled cones constituting 3% of the photoreceptors were lost by 3 months, as previously reported[19] (Figure 1A).

Received 21 March 2018; accepted 12 July 2018;
https://doi.org/10.1016/j.ymthe.2018.07.012.

Correspondence: Koji M. Nishiguchi, MD, PhD, FRCOphth, Associate Professor, Department of Advanced Ophthalmic Medicine, Tohoku University Graduate School of Medicine, 1-1 Seiryo-cho Aoba-ku Sendai-shi Miyagi-ken 980-8574, Japan.
E-mail: nishiguchi@oph.med.tohoku.ac.jp

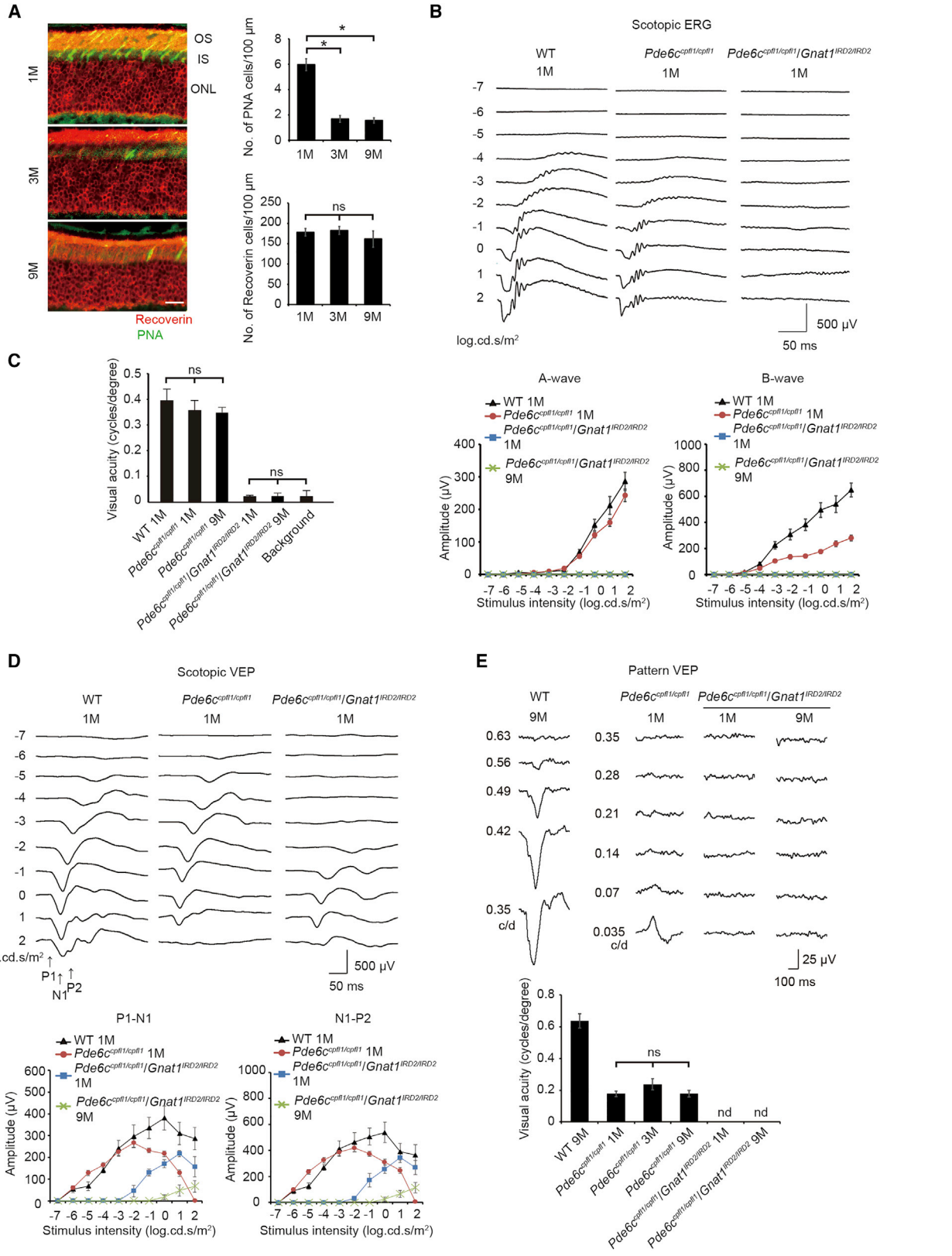

(legend on next page)

Structured functional assessment of the visual pathway revealed that the double mutants were essentially blind (Figures 1B–1E). No measurable visual response was detected by electroretinogram (ERG), reflecting severely compromised retinal function (Figure 1B). The optokinetic response (OKR; Figure 1C) predominantly reflects the function of the retinogeniculate projection, with a smaller contribution from the V1,[20] whereas the pattern visually evoked potential (pVEP; Figure 1E) primarily measures the function of the V1. These two functional assessments revealed no detectable visual acuity in the double mutants. Notably, the pVEP-measured acuity was lower (1 month, 0.177 ± 0.018 cycles per degree; 9 months, 0.178 ± 0.021, by ∼50%; Figure 1E) than the OKR-measured acuity (1 month, 0.361 ± 0.024 cycles per degree; 9 month, 0.350 ± 0.021 cycles per degree) in the sighted controls inborn with wild-type copies of rod-specific *Gnat1* (*Pde6c* $^{cpfl1/cpfl1}$ mice); conversely, pVEP-measured acuity was better than OKR-measured acuity in the wild-type mice (Figures 1C and 1E).

Meanwhile, the residual cortical responses were detected in the double mutants by flash VEP (fVEP), which is suitable for measuring the sensitivity and magnitude of the V1 response to light; however, the mice were severely desensitized by 4-log units, responding only to the brightest flashes (Figure 1D). Collectively, these data reveal that *Pde6c*$^{cpfl1/cpfl1}$*Gnat1*$^{IRD2/IRD2}$ mice have blinding congenital retinal dysfunction and that only the rod visual pathway allows for the reliable assessment of cortical plasticity in this model over an extended period of time. Importantly, these results also indicate that any measurable visual function detected by ERG, OKR, or pVEP following the treatment would likely be the consequence of therapeutic intervention.

Substantial Restoration of Rod-Mediated Visual Acuity Regardless of Age in *Pde6c*$^{cpfl1/cpfl1}$*Gnat1*$^{IRD2/IRD2}$ Mice

Using the blind double mutants, we tested the effect of adeno-associated virus (AAV)-mediated rod-specific *GNAT1* supplementation on the visual function. At 1 week after injection, the retinal expression of α-transducin encoded by *GNAT1* was confirmed by western blot analysis, confirming the quality of the subretinal therapeutic gene transfer (Figure 2A). *Pde6c*$^{cpfl1/cpfl1}$*Gnat1*$^{IRD2/IRD2}$ mice were then treated with the vector at 1, 3, 9, and 16 months. Following the treatment, ERG recordings revealed similar response amplitudes across the different time points for a-waves (generated mainly from the photoreceptors) and b-waves (derived mostly from the bipolar cells), yielding no differences in the rescue effects with a delay in treatment (Figure 2B). OKR, which also demonstrated similar visual acuity and contrast sensitivity across the different ages treated, indicated that the visual information was relayed via retinogeniculate projection without overt degradation with delayed intervention (Figure 2C). Importantly, even the cortical responses toward light probed by fVEP did not diminish with the delay (Figure 2D). Instead, the largest fVEP responses were observed in the oldest mice treated at 16 months for a few flash intensities (N1-P2; p = 0.0024, 0.006, and 0.0495 by ANOVA for stimulus of 0.0001, 0.001, and 0.01 cd/m^2, respectively).

These rather unexpected observations were convincingly backed up by the substantial restoration of rod-mediated visual acuity probed by pVEP for all ages treated (1, 3, and 9 months; Figure 2E), revealing spatial resolution thresholds that were indistinguishable from those of the controls born with the wild-type *Gnat1* gene (*Pde6c*$^{cpfl1/cpfl1}$ mice). Interestingly, we also observed an age-dependent increase in the pVEP amplitudes with delayed treatment (p = 0.0017, Jonckheere-Terpstra test for trend); pVEP amplitudes in these mice exceeded those of the *Pde6c*$^{cpfl1/cpfl1}$ mice of a similar age and were similar to the levels of wild-type mice. We also observed a similar restoration of rod-mediated visual acuity and an age-dependent increase in the pVEP amplitudes in mice with partly different (∼50%) genetic backgrounds (Figure S1), which were generated by crossing transgenic mice carrying *Arc* promoter-driven *dVenus* gene, i.e., *Tg(Arc-dVenus)*,[21] and the double mutants.

Restoration of Light-Dependent Transcription of *Arc* in Adult *Pde6c*$^{cpfl1/cpfl1}$*Gnat1*$^{IRD2/IRD2}$*-Tg(Arc-dVenus)* Mice

To provide molecular insights into the restored cortical activity, *Tg(Arc-dVenus)* mice, capable of tagging light-dependent neural

Figure 1. Blindness Accompanied by Progressive Cone Loss in *Pde6c*$^{cpfl1/cpfl1}$*Gnat1*$^{IRD2/IRD2}$ Mice

(A) Progressive loss of cone photoreceptors in *Pde6c*$^{cpfl1/cpfl1}$*Gnat1*$^{IRD2/IRD2}$ mice. Representative images (left panels) of the retina reveal PNA-positive cone inner and outer segments (green). PNA-positive cones indicated a reduction by 3 months, whereas recoverin-positive photoreceptors (red) remained constant (right panels; n = 5 for 1, 3, and 9 months). (B) Undetectable electroretinogram (ERG) responses in *Pde6c*$^{cpfl1/cpfl1}$*Gnat1*$^{IRD2/IRD2}$ mice. Representative images are shown of the ERG responses from wild-type (WT) controls, *Pde6c*$^{cpfl1/cpfl1}$ mice, and *Pde6c*$^{cpfl1/cpfl1}$*Gnat1*$^{IRD2/IRD2}$ mice at 1 month (upper traces). Amplitudes of a-waves and b-waves from WT mice (n = 5), *Pde6c*$^{cpfl1/cpfl1}$ mice (1 month, n = 6), and *Pde6c*$^{cpfl1/cpfl1}$*Gnat1*$^{IRD2/IRD2}$ mice (n = 6 for 1 and 9 months) were quantified (lower panels). (C) Undetectable optokinetic response (OKR) in *Pde6c*$^{cpfl1/cpfl1}$*Gnat1*$^{IRD2/IRD2}$ mice. Visual acuity of *Pde6c*$^{cpfl1/cpfl1}$ mice at 1 month (n = 4) and 9 months (n = 6) and WT controls (n = 6) were similar. Conversely, visual acuity in *Pde6c*$^{cpfl1/cpfl1}$*Gnat1*$^{IRD2/IRD2}$ mice at 1 month (n = 5) and 9 months (n = 6) was similar to the negative controls (background; n = 10). Visual acuity was measured at 100% contrast, and contrast sensitivity was measured with a fixed spatial resolution of 0.042 cycles per degree. (D) Severely desensitized flash visually evoked potential (fVEP) responses in *Pde6c*$^{cpfl1/cpfl1}$*Gnat1*$^{IRD2/IRD2}$ mice. Representative traces are shown of fVEP responses (upper traces) from WT controls, *Pde6c*$^{cpfl1/cpfl1}$ mice, and *Pde6c*$^{cpfl1/cpfl1}$*Gnat1*$^{IRD2/IRD2}$ mice at 1 month of age. Amplitudes of P1-N1 and N1-P2 from WT mice (n = 5), *Pde6c*$^{cpfl1/cpfl1}$ mice (1 month, n = 6), and *Pde6c*$^{cpfl1/cpfl1}$*Gnat1*$^{IRD2/IRD2}$ mice (n = 6 for 1 and 9 months) were quantified (lower panels). fVEP responses observed in *Pde6c*$^{cpfl1/cpfl1}$*Gnat1*$^{IRD2/IRD2}$ mice were desensitized by ∼4 log units. (E) Undetectable pattern VEP (pVEP) in *Pde6c*$^{cpfl1/cpfl1}$*Gnat1*$^{IRD2/IRD2}$ mice. Representative pVEP traces are shown from WT, *Pde6c*$^{cpfl1/cpfl1}$ (1 month), and *Pde6c*$^{cpfl1/cpfl1}$*Gnat1*$^{IRD2/IRD2}$ (1 and 9 months) mice (upper traces). No detectable pVEP was recorded for *Pde6c*$^{cpfl1/cpfl1}$*Gnat1*$^{IRD2/IRD2}$ mice (1 and 9 months; lower panel). n = 5, 6, 5, 5, 5, and 5 for WT, *Pde6c*$^{cpfl1/cpfl1}$ (1, 3, and 9 months), and *Pde6c*$^{cpfl1/cpfl1}$*Gnat1*$^{IRD2/IRD2}$ (1 and 9 months) mice, respectively. OS, outer segment; IS, inner segment; ONL, outer nuclear layer; No Tx, no treatment; ns, not significant. Data represent mean ± SEM. *ANOVA followed by post hoc test was carried out for (A) and (C), p < 0.05.

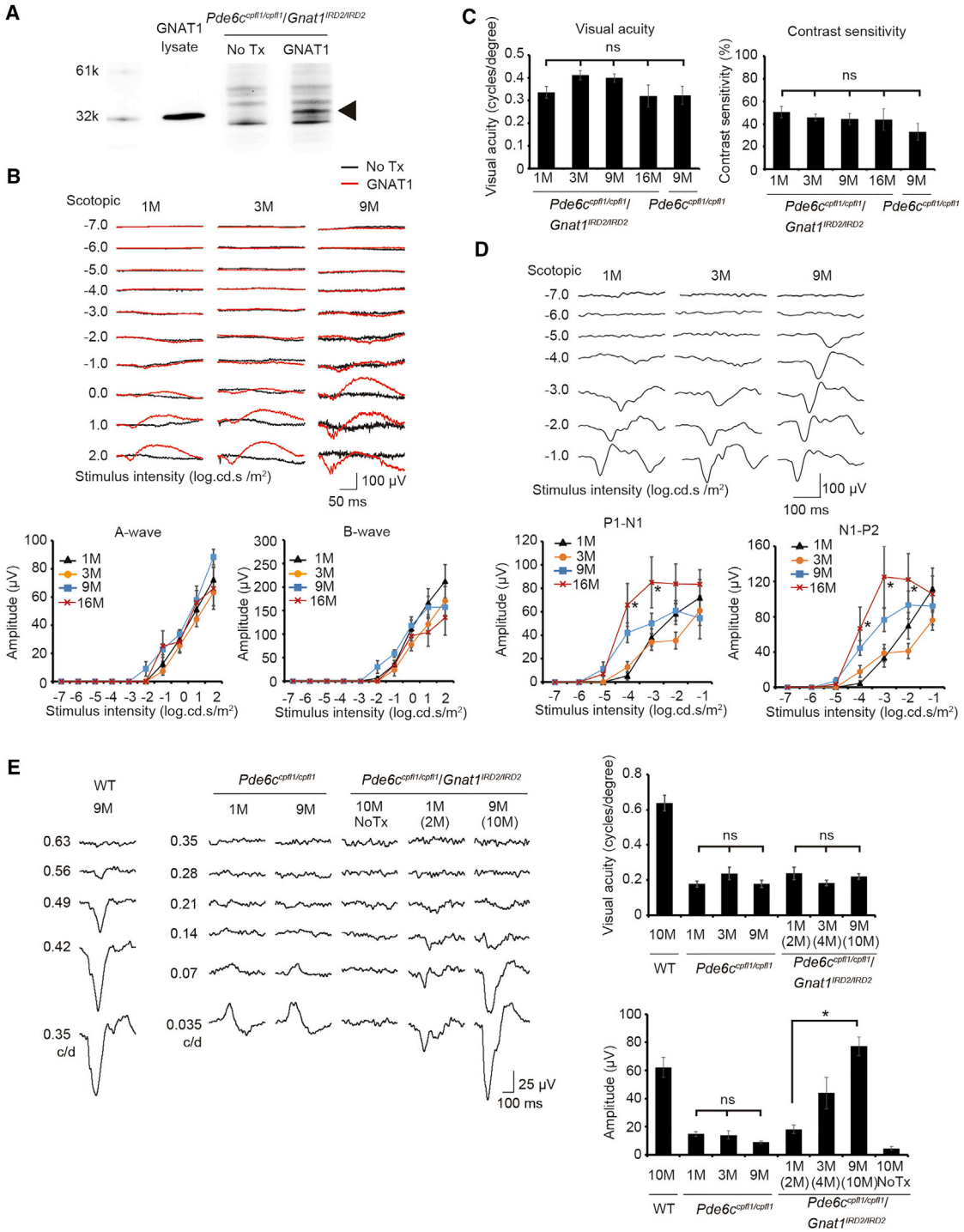

Figure 2. Substantial Restoration of Rod-Mediated Vision in Adult *Pde6c*$^{cpfl1/cpfl1}$*Gnat1*$^{IRD2/IRD2}$ Mice following *GNAT1* Supplementation

(A) Western blot revealing an immunoreactive band at 40 kilodalton (kd) corresponding to α-transducin (arrowhead) in the lysate from HEK293T cells and in the eye treated with AAV2/8.CMV.GNAT1 (GNAT1), but not in the contralateral untreated eye (No Tx). (B) Representative traces of ERG responses in adult *Pde6c*$^{cpfl1/cpfl1}$*Gnat1*$^{IRD2/IRD2}$ mice following *GNAT1* supplementation at 1, 3, and 9 months (upper traces). Quantification of a-wave and b-wave amplitudes in *Pde6c*$^{cpfl1/cpfl1}$*Gnat1*$^{IRD2/IRD2}$ mice following *GNAT1* supplementation (lower panels) is shown. Note that restored ERG responses were not different in mice treated at 1 month (n = 13), 3 months (n = 8), 9 months (n = 9), and 16 months (n = 6). (C) Restoration of visual acuity and contrast sensitivity in adult *Pde6c*$^{cpfl1/cpfl1}$*Gnat1*$^{IRD2/IRD2}$ mice following *GNAT1* supplementation. No difference in the restored OKR was detected when the mice were treated at 1 month (n = 11), 3 months (n = 9), 9 months (n = 13), and 16 months (n = 6) for both visual acuity (left) and

(legend continued on next page)

activity in the V1, were crossed with *Pde6c*$^{cpfl1/cpfl1}$*Gnat1*$^{IRD2/IRD2}$ mice to generate *Pde6c*$^{cpfl1/cpfl1}$*Gnat1*$^{IRD2/IRD2}$*-Tg(Arc-dVenus)* mice (triple-mutant mice). *Arc* is a neural activity-dependent regulator of excitatory synaptic transmission, with expression closely coupled to the plasticity of the V1.[22,23] Importantly, we have reported recently that *Arc* expression at the V1 is sufficient to extend the critical period of ocular dominance plasticity.[24] The use of this transgenic line allows for a more sensitive detection of the V1 light response over direct expression analysis of the Arc protein in the V1, which indicated high background expression in the dark (Figure S2). We used the triple-mutant mice unilaterally treated at 1 and 9 months to assess the light-induced immediate gene *Arc* transcription in the V1. It is known that 95% of the retinal projection in mice crosses the midline and terminates in the contralateral visual cortex. Consistent with the results of fVEP experiments (Figure 2D), western blot analysis revealed that *Arc* promoter-driven dVenus expression in the V1 contralateral to the treated eye was robust for triple mutants treated at 1 and 9 months compared with the ipsilateral V1 (Figures 3A and 3B). Notably, the expression of dVenus was greater in mice treated at 9 months than in those treated at 1 month. Furthermore, the histological comparison of the number of dVenus-positive cells at layer IV of the V1 contralateral to the treated eye was greater in mice treated at 16 months compared with those treated at 1 month (Figures 3B and 3C). This was also true when the dVenus count was corrected for the number of NeuN-positive cortical neurons. Meanwhile, a modest decline in the NeuN-positive cells with aging was detected between 1 and 16 months.

DISCUSSION

By focusing on the rod visual pathway, which undergoes minimal photoreceptor degeneration over time, we found that substantial restoration of rod-mediated visual acuity at the level of the visual cortex was possible in adult mice with congenital blindness due to retinal dystrophy. This was rather unexpected, as a delay in treatment has been reported to limit the recovery of OKR-measured visual acuity in a mouse model of congenital cone photoreceptor dysfunction.[25] However, other studies support our findings. First, dark-reared adult mice display slow development of visual acuity, reaching normal levels weeks after exposure to a visual scene.[26] Second, the gross formation of aspects of vision occurs intrinsically without visual input in mice,[26–28] although experience-dependent refinement of the supporting circuits also occurs.[29,30]

In humans, in addition to the inconsistent effectiveness of restoring visual acuity with retinal gene therapy for childhood blindness,[4,9–12] poor results in studies of treatments for eyes with congenital cataract[13–15] and corneal opacity[31,32] after years of blindness have strongly indicated that adequate visual input from the retina is required for the proper development of visual perception. However, as in mice, the retinotopic pattern of connectivity in the visual cortex is largely retained in congenitally blind adult patients.[33,34] Furthermore, an fMRI study of retinal dystrophy patients provided evidence for preservation of the anatomy of the light-responsive visual pathway,[6,35] and it showed increased sensitivity following gene therapy after many years of blindness.[6]

In retinal gene therapy trials, evidence for restoration of light sensitivity, a very simple visual function, has been consistently shown across different clinical trials; but, restoration of visual acuity, which requires more complex visual processing, showed inconsistent results. This has been attributed in part to limitations in the plasticity of the higher visual pathway, manifested as amblyopia.[3–6] As human visual acuity mainly reflects the state of the cone-photoreceptor pathway, which orchestrates a very complex visual circuit, poor recovery of visual acuity may be due to lost plasticity of this particular pathway. In other words, it is possible that the complex cone visual pathway is more hardwired, thus less plastic, than the simple rod visual pathway. Indeed, in a gene therapy trial,[10] recovery of visual acuity was better in a subset of patients with poorer visual acuity and extrafoveal fixation, i.e., in the area with both rods and cones, compared to patients with better acuity and foveal fixation, i.e., in the area with only cones.[10]

An alternative theory is that significant residual visual function, present before treatment in many patients, may have somehow restricted the recovery of visual acuity, in contrast with the mice used in this study, which had no measurable visual acuity. This theory arises from an observation in mice and humans. In the mouse model of congenital cone dysfunction, which displayed the features of amblyopia, there was only mild impairment of visual acuity.[25] Furthermore, a unique group of patients with severe, bilateral congenital cataract that was optically reconstructed later in life showed unexpectedly good recovery of visual function.[36] However, factors other than amblyopia may also explain the gap in visual outcomes in human gene therapy and the current mouse study. First, significant irreversible retinal degeneration, not clearly recognizable with *in vivo* imaging, could have been present in the enrolled patients in the gene therapy trials.[37] Therefore, limited visual acuity restoration in humans could also be attributed to retinal factors. Second, nystagmus is often present in patients, but not in mice, which could have confounded the finding of poor visual acuity restoration.[37]

contrast sensitivity (right). Visual acuity was measured at 100% contrast, and contrast sensitivity was measured with a fixed spatial resolution of 0.042 cycles per degree. (D) Representative traces of fVEP measurements revealing robust cortical response in adult *Pde6c*$^{cpfl1/cpfl1}$*Gnat1*$^{IRD2/IRD2}$ mice following *GNAT1* supplementation at 1, 3, and 9 months (upper traces). Quantification of P1-N1 and N1-P2 amplitudes indicate robust cortical response in adult *Pde6c*$^{cpfl1/cpfl1}$*Gnat1*$^{IRD2/IRD2}$ mice following *GNAT1* supplementation. n = 11, 8, 12, and 6 for 1, 3, 9, and 16 months, respectively (lower panels). (E) Representative traces of pVEP measurements revealing restoration of rod-mediated visual acuity in adult *Pde6c*$^{cpfl1/cpfl1}$*Gnat1*$^{IRD2/IRD2}$ mice following *GNAT1* supplementation at 1, 3, and 9 months (left). Quantification of visual acuity and N1-P2 amplitudes for 0.035 cycles/degree indicate robust cortical response (upper right) in adult *Pde6c*$^{cpfl1/cpfl1}$*Gnat1*$^{IRD2/IRD2}$ mice following *GNAT1* supplementation (lower right). A trend for age-dependent increases in N1-P2 amplitudes was observed ($p = 0.0017$). n = 11, 8, and 12 for 1, 3, and 9 months, respectively. Data represent the mean ± SEM; *$p < 0.05$; No Tx, no treatment; ns, not significant; c/d, cycles per degree; ANOVA followed by post hoc test was applied to (C) and (E) (visual acuity). Jonckheere-Terpstra trend test was applied in (E) (amplitudes).

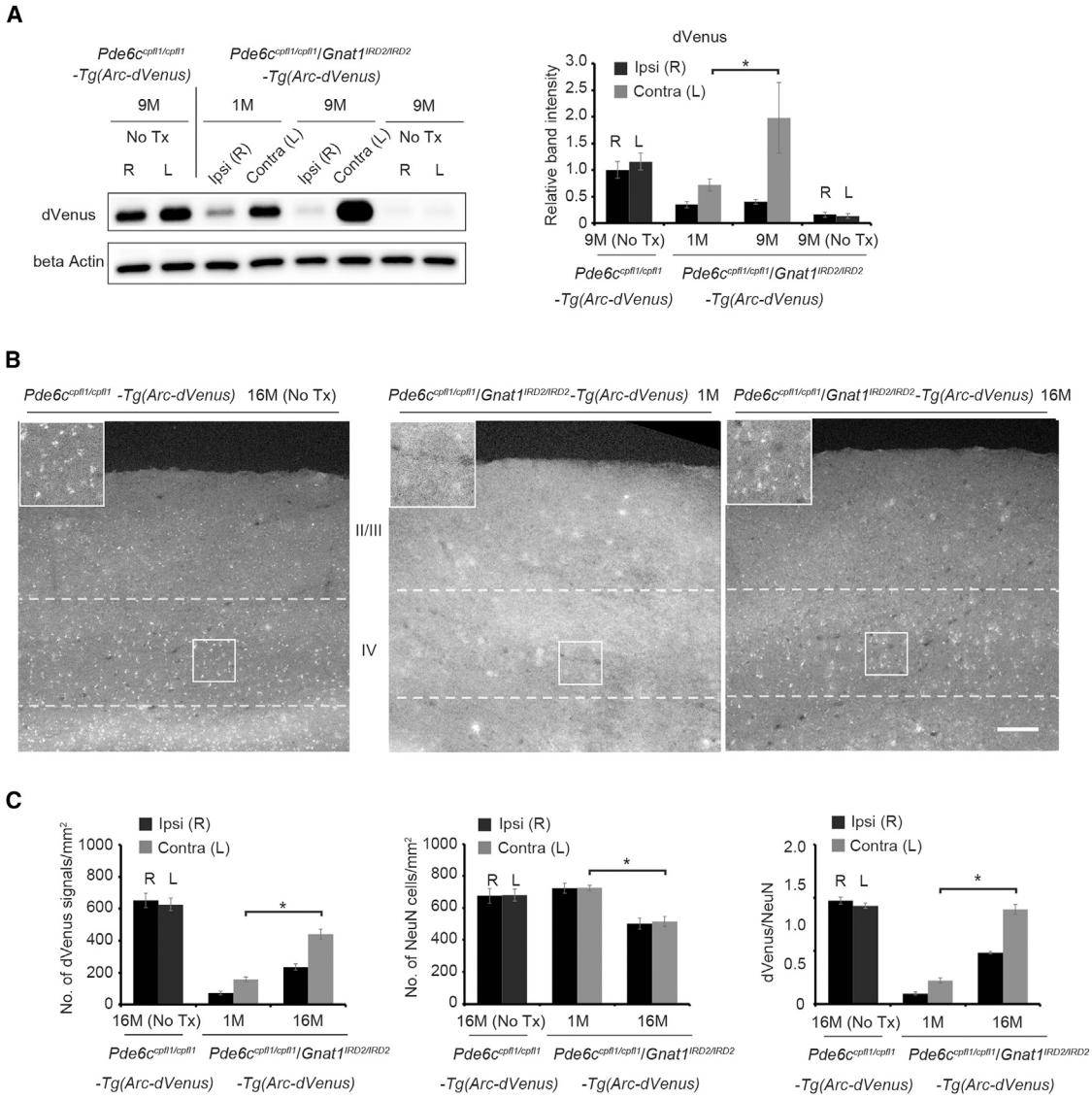

Figure 3. Restoration of Rod-Mediated *Arc* Transcription in the V1 of Adult *Pde6c*$^{cpfl1/cpfl1}$*Gnat1*$^{IRD2/IRD2}$*-Tg(Arc-dVenus)* Mice following *GNAT1* Supplementation

(A) Representative western blot image revealing robust light-induced expression of *Arc* promoter-driven d2-Venus after *GNAT1* supplementation in *Pde6c*$^{cpfl1/cpfl1}$ *Gnat1*$^{IRD2/IRD2}$*-Tg(Arc-dVenus)* mice at 1 and 9 months (left). Quantification of the western blot results for dVenus indicates light-induced expression of d2-Venus at the contralateral V1 in *Pde6c*$^{cpfl1/cpfl1}$*Gnat1*$^{IRD2/IRD2}$*-Tg(Arc-dVenus)* mice following AAV-mediated supplementation of *GNAT1* (right). n = 5, 10, 6, and 6 for 9-month *Pde6c*$^{cpfl1/cpfl1}$*Tg(Arc-dVenus)* mice and 1- and 9-month treated and 9-month untreated *Pde6c*$^{cpfl1/cpfl1}$*Gnat1*$^{IRD2/IRD2}$*-Tg(Arc-dVenus)* mice, respectively. (B) Representative histology images of cells positive for *Arc* promoter-driven dVenus expression at the V1 (layer IV). Images for the left hemisphere are revealed for 16-month untreated *Pde6c*$^{cpfl1/cpfl1}$*Tg(Arc-dVenus)* mice and 1- and 16-month treated *Pde6c*$^{cpfl1/cpfl1}$*Gnat1*$^{IRD2/IRD2}$*-Tg(Arc-dVenus)* mice. Note that the expression of dVenus is weak in *Pde6c*$^{cpfl1/cpfl1}$*Gnat1*$^{IRD2/IRD2}$*-Tg(Arc-dVenus)* mice treated at 1 month. The hemisphere evaluated is contralateral to the treated eye. Scale bar, 100 μm. (C) Quantification of the *Arc* promoter-driven dVenus and NeuN at layer IV. dVenus-positive cells were increased in layer IV of *Pde6c*$^{cpfl1/cpfl1}$*Gnat1*$^{IRD2/IRD2}$*-Tg(Arc-dVenus)* mice treated at 16 months (n = 5) compared with those treated at 1 month (n = 5; p = 0.00072; left). This remained true after correcting for NeuN density (p = 0.00030; right). Meanwhile, there was a modest decline in the number of NeuN-positive cells in mice treated at 16 months compared with those treated at 1 month (middle). Data represent the mean ± SEM; *p < 0.05; No Tx, no treatment; ns, not significant.

The relevance of our findings in the rod visual pathway to cone-mediated vision is unclear. It is difficult to verify this because progressive cone degeneration, commonly evident by ~1 month of age in the available models of severe cone dysfunction,[19,38,39] confounds the assessment of adult visual plasticity in the cone system. Nevertheless, our findings on the rod visual system are clinically significant on their

own, as the vast majority of patients with congenital blinding retinal dystrophy, e.g., Leber's congenital amaurosis, have visual acuity that falls below maximal rod-mediated vision (Snellen acuity of ~20/200),[40] particularly in adults.[41] Therefore, the present findings provide a rationale for the development of treatments for children and adults congenitally blinded by retinal dystrophies, even if the restoration of cone-mediated vision is impossible or unpredictable. Furthermore, rod photoreceptor transplantation may be able to successfully take advantage of the plastic rod visual pathway in advanced photoreceptor degeneration, which is observed in the majority of adults blinded early in life by retinal dystrophies.[42,43]

In *Pde6c*$^{cpfl1/cpfl1}$mice with rod-only function, visual acuity as tagged with OKR was consistently better than visual acuity as measured with pVEP. By contrast, visual acuity as measured with pVEP was better than visual acuity as tagged with OKR in wild-type mice in our study and in previous reports.[44,45] Therefore, it is possible that successful maturation of the rod-mediated visual pathway at the level of the visual cortex requires cone photoreceptor inputs, whereas this may be less important at the level of the retinogeniculate projection.

It is known that intrinsically photosensitive retinal ganglion cells (ipRGCs) mediate non-image-forming vision, including accessory visual functions such as the pupillary light reflex and circadian photo-entrainment using melanopsin.[46] The ipRGCs mainly project to the suprachiasmatic nucleus and other brain nuclei,[47] but evidence suggests that a subpopulation of ipRGCs also projects to the dorsal lateral geniculate nucleus and, thereby, contributes to image-forming vision.[48] In our study, the residual visual response, detected in response to the brightest fVEP flashes, in double-mutant mice lacking both rod and cone functions could have been mediated by the ipRGCs. However, the possible contribution of ipRGCs appears limited as ERG, OKR, and pVEP measurement showed no detectable response in the double mutants up to 9 months. In theory, these three tests should allow us to assess the effect of functional restoration of the rods on the downstream visual pathway without contamination from ipRGC input. Furthermore, since the treated eyes had robust rod function in ERG testing and had restored visual acuity that was indistinguishable from the control mice (which were born with normal rod function), it is unlikely that adaptational changes in the ipRGC pathway to blindness made a significant contribution to the restored vision.

In conclusion, we found that substantial restoration of rod-mediated visual acuity is in principle possible, at least at the level of the visual cortex, in adult mice born with blinding retinal dysfunction. The study raises the possibility of neuroplasticity in adults, as well as children, with congenital blindness due to retinal dystrophies.

MATERIALS AND METHODS

Animals

Pde6c$^{cpfl1/cpfl1}$*Gnat1*$^{IRD2/IRD2}$ mice were generated by crossing the rod-defective *Gnat1*$^{IRD2/IRD2}$ mice (Takeda, Japan)[16] and cone-defective *Pde6c* $^{cpfl1/cpfl1}$ mice (Jackson Laboratory, Bar Harbor, ME).[19] During the course of crossbreeding, litters of *Pde6c*$^{cpfl1/cpfl1}$ *Gnat1*$^{IRD2/IRD2}$ mice that had no mutation in either of the genes (*Pde6c* and *Gnat1*) were isolated and maintained separately as isotype wild-type controls and used for experiments. *Tg(Arc-dVenus)* mice on a C56BL/6 background were provided from the University of Tokyo (H.B., H.O., and S.T.-K.) and were crossed with *Pde6c*$^{cpfl1/cpfl1}$ *Gnat1*$^{IRD2/IRD2}$ mice to generate *Pde6c*$^{cpfl1/cpfl1}$*Gnat1*$^{IRD2/IRD2}$-*Tg(Arc-dVenus)* mice. The surgical procedures were performed by the intraperitoneal administration of anesthetics (a mixture of ketamine at 37.5 mg/kg and medetomidine at 0.625 mg/kg). After the surgery, the effect of medetomidine was reversed by the intraperitoneal injection of 1.25 mg/kg atipamezole. For experiments using*Tg(Arc-dVenus)* mice, dark-adapted animals were kept in the dark for 24 hr before use. Light-adapted animals were further kept under constant light (120 cd/m^2) for 6 hr after dark adaptation for 48 hr before use.

Mice were handled and maintained in accordance with the ARVO Statement guidelines for the Use of Animals in Ophthalmic and Vision Research and the Declaration of Helsinki and the Tohoku University guidelines for the care and use of animals. All experimental procedures were conducted after approval by the ethics committees for the animal experiments at Tohoku University Graduate School of Medicine and the University of Tokyo, Graduate School of Medicine.

AAV Vectors and Gene Therapy

To construct pCMV.hGNAT1, human GNAT1 cDNA (KIEE3139; Promega, Madison, WI) was inserted downstream of the cytomegalovirus (CMV) promoter into a pAAV-MCS expression vector (Cell Biolabs, San Diego, CA). Then, recombinant AAV (rAAV)2/8. CMV.hGNAT1 was generated and purified following a method described previously.[49] The viral vector was reconstituted at 1.0 × 10^{12} genome copy/mL, and it was injected into the subretinal space (2.0 μL/injection; total of 4.0 μL/eye) at the superior and inferior hemispheres of the anesthetized mice aged 1–16 months, which corresponds roughly to the ages between 3 and 53 years in humans.[50] The dose was the same in all experiments involving subretinal injection of AAV in this study.

Electrophysiological Assessment

ERG and fVEP readings were recorded from both eyes and both occipital lobes, as previously described in detail.[51] ERG was recorded as previously described,[51] 1 week after rAAV2/8 injection. Surgical implantation of the VEP electrodes was carried out at 18 days after the injection, followed by fVEP recording 1 week later. pVEP readings were recorded by placing a 19-in monitor (S1933; EIZO, Hakusan, Japan) placed parallel to and 16 cm away from the plane of the stimulated eye and using the same electrode system for measuring fVEP. The contralateral eye was completely covered to ensure that no light entered this eye. Patterns of black (3 cd/m^2) and white (159 cd/m^2) vertical stripes of equal width with different spatial resolutions (0.63, 0.56, 0.49, 0.42, and 0.35 cycles per degree for the wild-type mice and 0.35, 0.28, 0.21, 0.14, 0.07, and 0.035 cycles per degree for

the others) projected onto the monitor using a stimulator (DATAPixx; VPixx Technologies, Montreal, Canada) were abruptly reversed at 2 Hz. The extracted electrical responses were band-pass filtered at 0.3 and 50 Hz, and the responses were averaged 400 times for each stimulus. The amplitudes for the positive peak (N1-P2) were plotted vertically as a function of the log spatial resolution of the stimulus (horizontally), and four data points were used to obtain a regression line (calculated by linear extrapolation) for each mouse. pVEP-measured visual acuity was defined as the intersection of the regression line and horizontal line representing the background noise (2.80 μV).

OKR Measurement Using Optomotry

Visual acuities and contrast sensitivity were measured 2 weeks after the AAV injection by observing the OKRs of mice to the rotating sinusoidal gratings (Optomotry; Cerebral Mechanics, Lethbridge, Canada), as described previously.[52] This test yields independent measures of right and left eye acuity based on the unequal sensitivities to pattern rotation direction, as the motion in the temporal-to-nasal direction dominates the tracking response.[53] Mice were housed under standard lighting conditions for at least 6 hr before they were placed in the recording chamber. Visual acuity and contrast sensitivity reported for each eye represent the averages of four trials conducted on 4 consecutive days.

Western Blot Analysis

Western blot analysis was carried out as described previously.[54] In brief, the isolated mouse retinas were lysed in radio-immunoprecipitation assay (RIPA) buffer supplemented with a protease inhibitor by sonication on ice. Total protein concentration was measured with the Pierce BCA protein assay kit (Thermo Fisher Scientific, Waltham, MA). Mouse retinal proteins (15 mg each) were separated by SDS-PAGE on Mini-PROTEAN TGX Precast gels (Bio-Rad, Hercules, CA), and they were transferred to the polyvinylidene fluoride (PVDF) membranes. The membranes were blocked in 5% milk in PBS with Tween 20 (PBS-T) for 1 hr and then incubated with antibodies against transducin alpha (ab74059, 1/2,000; Abcam, Cambridge, UK), GFP (598, 1/2,000; MBL, Nagoya, Japan), and beta-actin (F5316, 1/2,000; Sigma-Aldrich, St. Louis, MO), for 1 hr. The membranes were then washed thrice with PBS-T and incubated with horseradish peroxidase (HRP)-conjugated anti-rabbit immunoglobulin G (IgG) antibodies or anti-mouse IgG antibodies for 1 hr, and they were then washed four times with PBS-T. The immunogenic reaction was detected by enhanced chemiluminescence (ECL).

Immunohistochemistry

Immunohistochemistry of the retina was performed as described previously.[54] Eyes were fixed in 4% paraformaldehyde, embedded in the optimal cutting temperature (OCT) compound, and sectioned using a cryostat. The sections were blocked with 5% donkey serum for 30 min, incubated with rabbit antirecoverin antibodies (AB5585, 1/20,000; Millipore) for 1 hr, and were then stained with an appropriate secondary antibody (anti-rabbit Alexa Fluor 488) and DAPI for an additional 45 min. Images were acquired on a Zeiss LSM780 confocal microscope (Carl Zeiss, Jena, Germany). Stained cells in the inner nuclear layer and the outer nuclear layer were counted in a 100-μm area on each side of the optic nerve, under a 20× objective in three sections from each retina, and were averaged.

For the histological assessment of the visual cortex, brains were removed from the skull after cervical dislocation. After the frontal lobe was cut off, the plane of the cut brain was placed in the bottom of an aluminum foil cup where it was frozen using OCT compound on a dry ice block. Coronal sections, 18 μm in thickness and between −3.0 and ∼−3.2 mm from the bregma, were cut using a cryostat (Leica CM3050 S; Leica, Nussloch, Germany). The cryosections were fixed using 4% paraformaldehyde (PFA) and permeabilized with 0.5% polyoxyethylene in PBS. The sections were blocked with 5% donkey serum in Tween-PBS for 40 min and incubated with a primary antibody against NeuN (MAB377, 1:500; Millipore) at room temperature for 1 hr. After washing with Tween-PBS, the sections were incubated with Alexa Fluor 568-conjugated donkey anti-mouse IgG antibody (1/500; Thermo Fisher Scientific) in blocking buffer at room temperature for an additional 1 hr. The sections were then mounted on Vectashield mounting media containing DAPI. Images were acquired using a 10× objective on a Zeiss LSM780 confocal microscope (Carl Zeiss). The quantification of the *Arc*-driven dVenus-positive cells in layer IV was conducted as reported previously with slight modification.[24] The background of the image was thresholded to the same level, and *Arc*-positive cells in layer IV were quantified. Layer IV in the visual cortex was determined by measuring 250 μm ventral to the dorsal cortical surface and 2.3 mm lateral to the longitudinal cerebral fissure. Stained cells in layer IV were counted in a 200-μm-tall × 500-μm-wide area in four sections from each hemisphere.

Statistical Analysis

Differences between the two groups were assessed using the unpaired Student's t test. For assessing the differences between three or more groups, ANOVA was used. If the ANOVA was significant, the Tukey test was used as a post hoc test. Jonckheere-Terpstra trend test was applied to test for an increasing or decreasing trend. Statistical analysis was performed by JMP (SAS Institute, Cary, NC). All values are expressed as the mean ± SEM and $p < 0.05$ was considered statistically significant.

SUPPLEMENTAL INFORMATION

Supplemental Information includes two figures and can be found with this article online at https://doi.org/10.1016/j.ymthe.2018.07.012.

AUTHOR CONTRIBUTIONS

K.M.N. designed the experiments. K.M.N. and K.F. performed the experiments and analyzed the data. N.T. and H.K. helped with the animal experiments. S.T.-K., H.O., and H.B. provided *Arc-dVenus* transgenic mice and related data. K.M.N. wrote the manuscript. K.M.N. and T.N. obtained the funding.

ACKNOWLEDGMENTS

This work was supported in part by JSPS KAKENHI Grants-in-Aid for Scientific Research C (K.M.N., 16K11315) and Japan Agency for Medical Research and Development (K.M.N., 17ek0109213h0001) as well as by the Japanese Retinitis Pigmentosa Society (K.M.N.) and Alcon Pharma (K.M.N. and T.N.). The manuscript was edited by a professional English editing service (Enago, Tokyo, Japan; https://www.enago.jp/).

REFERENCES

1. Attebo, K., Mitchell, P., Cumming, R., Smith, W., Jolly, N., and Sparkes, R. (1998). Prevalence and causes of amblyopia in an adult population. Ophthalmology *105*, 154–159.

2. Liew, G., Michaelides, M., and Bunce, C. (2014). A comparison of the causes of blindness certifications in England and Wales in working age adults (16-64 years), 1999-2000 with 2009-2010. BMJ Open *4*, e004015.

3. Bainbridge, J.W., Smith, A.J., Barker, S.S., Robbie, S., Henderson, R., Balaggan, K., Viswanathan, A., Holder, G.E., Stockman, A., Tyler, N., et al. (2008). Effect of gene therapy on visual function in Leber's congenital amaurosis. N. Engl. J. Med. *358*, 2231–2239.

4. Maguire, A.M., High, K.A., Auricchio, A., Wright, J.F., Pierce, E.A., Testa, F., Mingozzi, F., Bennicelli, J.L., Ying, G.S., Rossi, S., et al. (2009). Age-dependent effects of RPE65 gene therapy for Leber's congenital amaurosis: a phase 1 dose-escalation trial. Lancet *374*, 1597–1605.

5. MacLaren, R.E. (2016). Benefits of gene therapy for both eyes. Lancet *388*, 635–636.

6. Ashtari, M., Cyckowski, L.L., Monroe, J.F., Marshall, K.A., Chung, D.C., Auricchio, A., Simonelli, F., Leroy, B.P., Maguire, A.M., Shindler, K.S., and Bennett, J. (2011). The human visual cortex responds to gene therapy-mediated recovery of retinal function. J. Clin. Invest. *121*, 2160–2168.

7. Maguire, A.M., Simonelli, F., Pierce, E.A., Pugh, E.N., Jr., Mingozzi, F., Bennicelli, J., Banfi, S., Marshall, K.A., Testa, F., Surace, E.M., et al. (2008). Safety and efficacy of gene transfer for Leber's congenital amaurosis. N. Engl. J. Med. *358*, 2240–2248.

8. Cideciyan, A.V., Aleman, T.S., Boye, S.L., Schwartz, S.B., Kaushal, S., Roman, A.J., Pang, J.J., Sumaroka, A., Windsor, E.A., Wilson, J.M., et al. (2008). Human gene therapy for RPE65 isomerase deficiency activates the retinoid cycle of vision but with slow rod kinetics. Proc. Natl. Acad. Sci. USA *105*, 15112–15117.

9. Bainbridge, J.W., Mehat, M.S., Sundaram, V., Robbie, S.J., Barker, S.E., Ripamonti, C., Georgiadis, A., Mowat, F.M., Beattie, S.G., Gardner, P.J., et al. (2015). Long-term effect of gene therapy on Leber's congenital amaurosis. N. Engl. J. Med. *372*, 1887–1897.

10. Jacobson, S.G., Cideciyan, A.V., Ratnakaram, R., Heon, E., Schwartz, S.B., Roman, A.J., Peden, M.C., Aleman, T.S., Boye, S.L., Sumaroka, A., et al. (2012). Gene therapy for leber congenital amaurosis caused by RPE65 mutations: safety and efficacy in 15 children and adults followed up to 3 years. Arch. Ophthalmol. *130*, 9–24.

11. Russell, S., Bennett, J., Wellman, J.A., Chung, D.C., Yu, Z.F., Tillman, A., Wittes, J., Pappas, J., Elci, O., McCague, S., et al. (2017). Efficacy and safety of voretigene neparvovec (AAV2-hRPE65v2) in patients with RPE65-mediated inherited retinal dystrophy: a randomised, controlled, open-label, phase 3 trial. Lancet *390*, 849–860.

12. Bennett, J., Wellman, J., Marshall, K.A., McCague, S., Ashtari, M., DiStefano-Pappas, J., Elci, O.U., Chung, D.C., Sun, J., Wright, J.F., et al. (2016). Safety and durability of effect of contralateral-eye administration of AAV2 gene therapy in patients with childhood-onset blindness caused by RPE65 mutations: a follow-on phase 1 trial. Lancet *388*, 661–672.

13. Birch, E.E., and Stager, D.R. (1996). The critical period for surgical treatment of dense congenital unilateral cataract. Invest. Ophthalmol. Vis. Sci. *37*, 1532–1538.

14. Lewis, T.L., and Maurer, D. (2005). Multiple sensitive periods in human visual development: evidence from visually deprived children. Dev. Psychobiol. *46*, 163–183.

15. Birch, E.E., Cheng, C., Stager, D.R., Jr., Weakley, D.R., Jr., and Stager, D.R., Sr. (2009). The critical period for surgical treatment of dense congenital bilateral cataracts. J. AAPOS *13*, 67–71.

16. Miyamoto, M., Aoki, M., Hirai, K., Sugimoto, S., Kawasaki, K., and Imai, R. (2010). A nonsense mutation in Gnat1, encoding the alpha subunit of rod transducin, in spontaneous mouse models of retinal dysfunction. Exp. Eye Res. *90*, 63–69.

17. Miyamoto, M., Aoki, M., Sugimoto, S., Kawasaki, K., and Imai, R. (2010). IRD1 and IRD2 mice, naturally occurring models of hereditary retinal dysfunction, show late-onset and progressive retinal degeneration. Curr. Eye Res. *35*, 137–145.

18. Miyamoto, M., Imai, R., Sugimoto, S., Aoki, M., Nagai, H., and Ando, T. (2006). Visual electrophysiological features of two naturally occurring mouse models with retinal dysfunction. Curr. Eye Res. *31*, 329–335.

19. Chang, B., Grau, T., Dangel, S., Hurd, R., Jurklies, B., Sener, E.C., Andreasson, S., Dollfus, H., Baumann, B., Bolz, S., et al. (2009). A homologous genetic basis of the murine cpfl1 mutant and human achromatopsia linked to mutations in the PDE6C gene. Proc. Natl. Acad. Sci. USA *106*, 19581–19586.

20. Prusky, G.T., and Douglas, R.M. (2004). Characterization of mouse cortical spatial vision. Vision Res. *44*, 3411–3418.

21. Mikuni, T., Uesaka, N., Okuno, H., Hirai, H., Deisseroth, K., Bito, H., and Kano, M. (2013). Arc/Arg3.1 is a postsynaptic mediator of activity-dependent synapse elimination in the developing cerebellum. Neuron *78*, 1024–1035.

22. Gao, M., Sossa, K., Song, L., Errington, L., Cummings, L., Hwang, H., Kuhl, D., Worley, P., and Lee, H.K. (2010). A specific requirement of Arc/Arg3.1 for visual experience-induced homeostatic synaptic plasticity in mouse primary visual cortex. J. Neurosci. *30*, 7168–7178.

23. Tagawa, Y., Kanold, P.O., Majdan, M., and Shatz, C.J. (2005). Multiple periods of functional ocular dominance plasticity in mouse visual cortex. Nat. Neurosci. *8*, 380–388.

24. Jenks, K.R., Kim, T., Pastuzyn, E.D., Okuno, H., Taibi, A.V., Bito, H., Bear, M.F., and Shepherd, J.D. (2017). Arc restores juvenile plasticity in adult mouse visual cortex. Proc. Natl. Acad. Sci. USA *114*, 9182–9187.

25. Carvalho, L.S., Xu, J., Pearson, R.A., Smith, A.J., Bainbridge, J.W., Morris, L.M., Fliesler, S.J., Ding, X.Q., and Ali, R.R. (2011). Long-term and age-dependent restoration of visual function in a mouse model of CNGB3-associated achromatopsia following gene therapy. Hum. Mol. Genet. *20*, 3161–3175.

26. Kang, E., Durand, S., LeBlanc, J.J., Hensch, T.K., Chen, C., and Fagiolini, M. (2013). Visual acuity development and plasticity in the absence of sensory experience. J. Neurosci. *33*, 17789–17796.

27. Ko, H., Mrsic-Flogel, T.D., and Hofer, S.B. (2014). Emergence of feature-specific connectivity in cortical microcircuits in the absence of visual experience. J. Neurosci. *34*, 9812–9816.

28. Hagihara, K.M., Murakami, T., Yoshida, T., Tagawa, Y., and Ohki, K. (2015). Neuronal activity is not required for the initial formation and maturation of visual selectivity. Nat. Neurosci. *18*, 1780–1788.

29. Mizuno, H., Hirano, T., and Tagawa, Y. (2007). Evidence for activity-dependent cortical wiring: formation of interhemispheric connections in neonatal mouse visual cortex requires projection neuron activity. J. Neurosci. *27*, 6760–6770.

30. Ishikawa, A.W., Komatsu, Y., and Yoshimura, Y. (2014). Experience-dependent emergence of fine-scale networks in visual cortex. J. Neurosci. *34*, 12576–12586.

31. Levin, N., Dumoulin, S.O., Winawer, J., Dougherty, R.F., and Wandell, B.A. (2010). Cortical maps and white matter tracts following long period of visual deprivation and retinal image restoration. Neuron *65*, 21–31.

32. Ackroyd, C., Humphrey, N.K., and Warrington, E.K. (1974). Lasting effects of early blindness. A case study. Q. J. Exp. Psychol. *26*, 114–124.

33. Striem-Amit, E., Ovadia-Caro, S., Caramazza, A., Margulies, D.S., Villringer, A., and Amedi, A. (2015). Functional connectivity of visual cortex in the blind follows retinotopic organization principles. Brain *138*, 1679–1695.

34. Bock, A.S., Binda, P., Benson, N.C., Bridge, H., Watkins, K.E., and Fine, I. (2015). Resting-State Retinotopic Organization in the Absence of Retinal Input and Visual Experience. J. Neurosci. *35*, 12366–12382.

35. Aguirre, G.K., Komáromy, A.M., Cideciyan, A.V., Brainard, D.H., Aleman, T.S., Roman, A.J., Avants, B.B., Gee, J.C., Korczykowski, M., Hauswirth, W.W., et al. (2007). Canine and human visual cortex intact and responsive despite early retinal blindness from RPE65 mutation. PLoS Med. *4*, e230.

36. Kalia, A., Lesmes, L.A., Dorr, M., Gandhi, T., Chatterjee, G., Ganesh, S., Bex, P.J., and Sinha, P. (2014). Development of pattern vision following early and extended blindness. Proc. Natl. Acad. Sci. USA *111*, 2035–2039.

37. Jacobson, S.G., Aleman, T.S., Cideciyan, A.V., Roman, A.J., Sumaroka, A., Windsor, E.A., Schwartz, S.B., Heon, E., and Stone, E.M. (2009). Defining the residual vision in leber congenital amaurosis caused by RPE65 mutations. Invest. Ophthalmol. Vis. Sci. *50*, 2368–2375.

38. Chang, B., Dacey, M.S., Hawes, N.L., Hitchcock, P.F., Milam, A.H., Atmaca-Sonmez, P., Nusinowitz, S., and Heckenlively, J.R. (2006). Cone photoreceptor function loss-3, a novel mouse model of achromatopsia due to a mutation in Gnat2. Invest. Ophthalmol. Vis. Sci. *47*, 5017–5021.

39. Michalakis, S., Geiger, H., Haverkamp, S., Hofmann, F., Gerstner, A., and Biel, M. (2005). Impaired opsin targeting and cone photoreceptor migration in the retina of mice lacking the cyclic nucleotide-gated channel CNGA3. Invest. Ophthalmol. Vis. Sci. *46*, 1516–1524.

40. Walia, S., Fishman, G.A., Jacobson, S.G., Aleman, T.S., Koenekoop, R.K., Traboulsi, E.I., Weleber, R.G., Pennesi, M.E., Heon, E., Drack, A., et al. (2010). Visual acuity in patients with Leber's congenital amaurosis and early childhood-onset retinitis pigmentosa. Ophthalmology *117*, 1190–1198.

41. Paunescu, K., Wabbels, B., Preising, M.N., and Lorenz, B. (2005). Longitudinal and cross-sectional study of patients with early-onset severe retinal dystrophy associated with RPE65 mutations. Graefes Arch. Clin. Exp. Ophthalmol. *243*, 417–426.

42. Singh, M.S., Charbel Issa, P., Butler, R., Martin, C., Lipinski, D.M., Sekaran, S., Barnard, A.R., and MacLaren, R.E. (2013). Reversal of end-stage retinal degeneration and restoration of visual function by photoreceptor transplantation. Proc. Natl. Acad. Sci. USA *110*, 1101–1106.

43. Barber, A.C., Hippert, C., Duran, Y., West, E.L., Bainbridge, J.W., Warre-Cornish, K., Luhmann, U.F., Lakowski, J., Sowden, J.C., Ali, R.R., and Pearson, R.A. (2013). Repair of the degenerate retina by photoreceptor transplantation. Proc. Natl. Acad. Sci. USA *110*, 354–359.

44. Prusky, G.T., Alam, N.M., Beekman, S., and Douglas, R.M. (2004). Rapid quantification of adult and developing mouse spatial vision using a virtual optomotor system. Invest. Ophthalmol. Vis. Sci. *45*, 4611–4616.

45. Ridder, W.H., 3rd, and Nusinowitz, S. (2006). The visual evoked potential in the mouse–origins and response characteristics. Vision Res. *46*, 902–913.

46. Hattar, S., Lucas, R.J., Mrosovsky, N., Thompson, S., Douglas, R.H., Hankins, M.W., Lem, J., Biel, M., Hofmann, F., Foster, R.G., and Yau, K.W. (2003). Melanopsin and rod-cone photoreceptive systems account for all major accessory visual functions in mice. Nature *424*, 76–81.

47. Hattar, S., Liao, H.W., Takao, M., Berson, D.M., and Yau, K.W. (2002). Melanopsin-containing retinal ganglion cells: architecture, projections, and intrinsic photosensitivity. Science *295*, 1065–1070.

48. Ecker, J.L., Dumitrescu, O.N., Wong, K.Y., Alam, N.M., Chen, S.K., LeGates, T., Renna, J.M., Prusky, G.T., Berson, D.M., and Hattar, S. (2010). Melanopsin-expressing retinal ganglion-cell photoreceptors: cellular diversity and role in pattern vision. Neuron *67*, 49–60.

49. Fujita, K., Nishiguchi, K.M., Yokoyama, Y., Tomiyama, Y., Tsuda, S., Yasuda, M., Maekawa, S., and Nakazawa, T. (2015). In vivo cellular imaging of various stress/response pathways using AAV following axonal injury in mice. Sci. Rep. *5*, 18141.

50. Dutta, S., and Sengupta, P. (2016). Men and mice: Relating their ages. Life Sci. *152*, 244–248.

51. Tomiyama, Y., Fujita, K., Nishiguchi, K.M., Tokashiki, N., Daigaku, R., Tabata, K., Sugano, E., Tomita, H., and Nakazawa, T. (2016). Measurement of Electroretinograms and Visually Evoked Potentials in Awake Moving Mice. PLoS ONE *11*, e0156927.

52. Nishiguchi, K.M., Carvalho, L.S., Rizzi, M., Powell, K., Holthaus, S.M., Azam, S.A., Duran, Y., Ribeiro, J., Luhmann, U.F., Bainbridge, J.W., et al. (2015). Gene therapy restores vision in rd1 mice after removal of a confounding mutation in Gpr179. Nat. Commun. *6*, 6006.

53. Douglas, R.M., Alam, N.M., Silver, B.D., McGill, T.J., Tschetter, W.W., and Prusky, G.T. (2005). Independent visual threshold measurements in the two eyes of freely moving rats and mice using a virtual-reality optokinetic system. Vis. Neurosci. *22*, 677–684.

54. Fujita, K., Nishiguchi, K.M., Shiga, Y., and Nakazawa, T. (2017). Spatially and Temporally Regulated *NRF2* Gene Therapy Using *Mcp-1* Promoter in Retinal Ganglion Cell Injury. Mol. Ther. Methods Clin. Dev. *5*, 130–141.

YMTHE, Volume *26*

Supplemental Information

Retained Plasticity and Substantial Recovery of Rod-Mediated Visual Acuity at the Visual Cortex in Blind Adult Mice with Retinal Dystrophy

Koji M. Nishiguchi, Kosuke Fujita, Naoyuki Tokashiki, Hiroshi Komamura, Sayaka Takemoto-Kimura, Hiroyuki Okuno, Haruhiko Bito, and Toru Nakazawa

Supplementary Materials

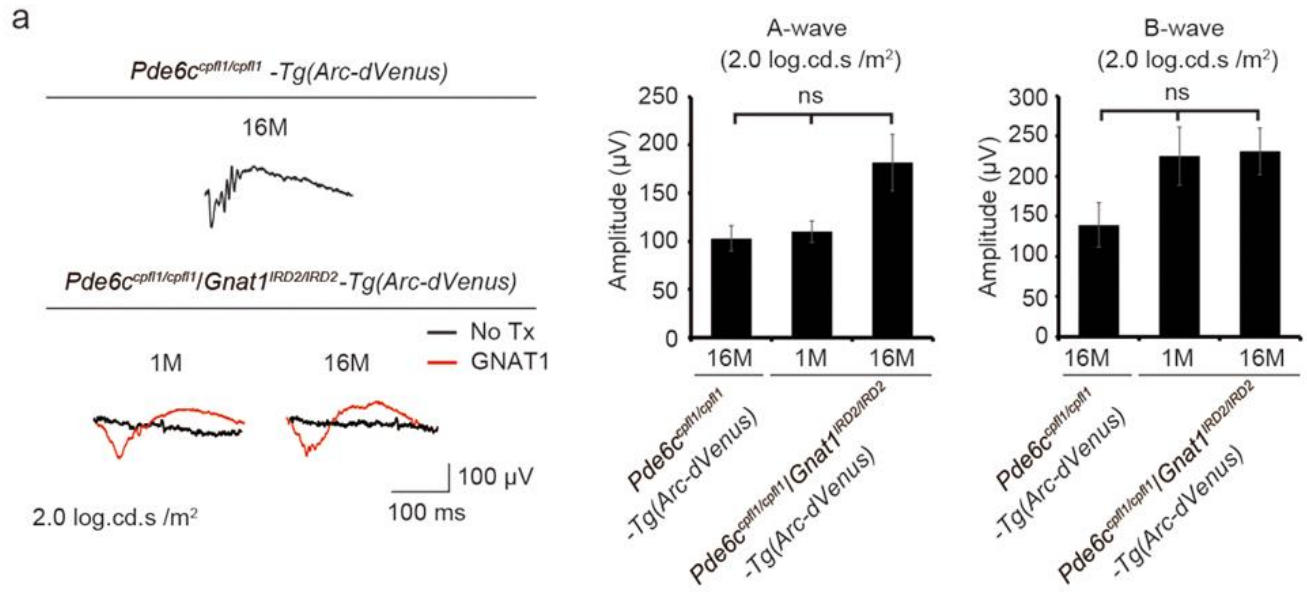

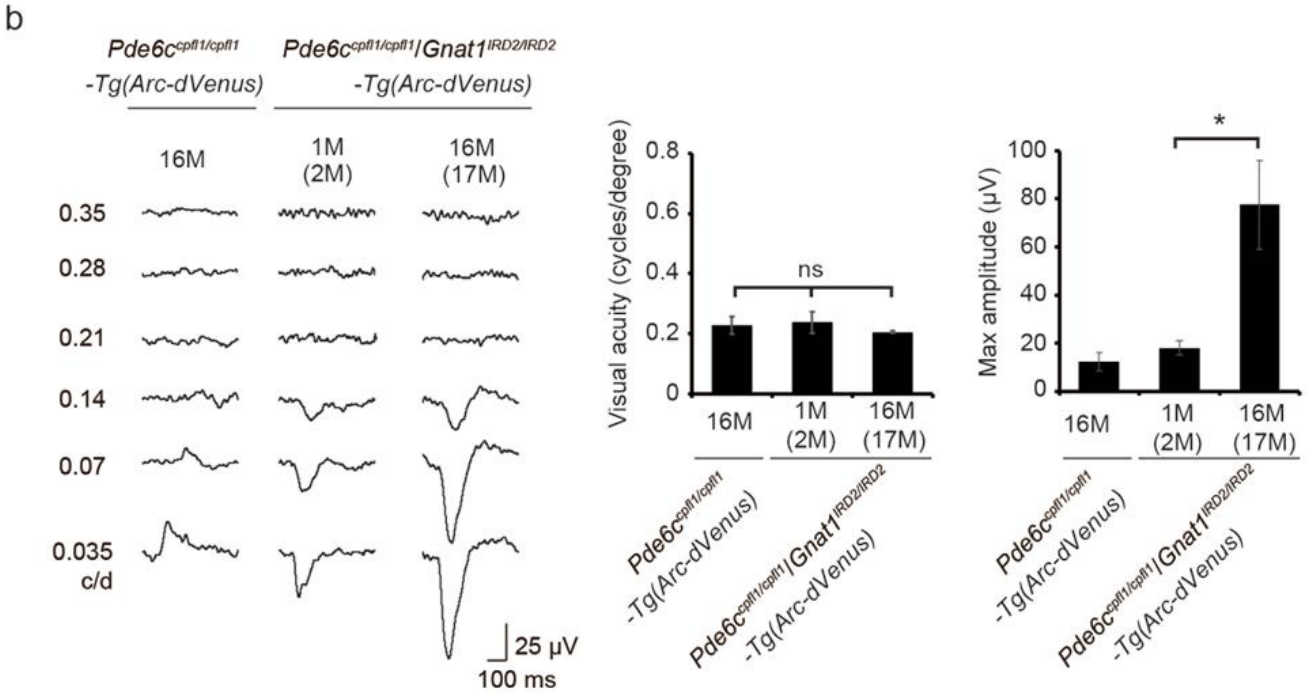

Supplementary Figure S1. Delayed treatment and increased pVEP amplitudes in *Pde6c$^{cpfl1/cpfl1}$Gnat1$^{IRD2/IRD2}$-Tg(Arc-dVenus)* mice.

a. Similar functional restoration of the retina in *Pde6c$^{cpfl1/cpfl1}$Gnat1$^{IRD2/IRD2}$-Tg(Arc-dVenus)* mice treated at 1 month and 16 months. Notably, a-wave and b-wave amplitudes were not different between the two groups (N = 5 and 4 for 1 month and 9 months; ANOVA).

b. pVEP revealed larger amplitudes in mice treated at 16 months (N = 4) compared with those treated at 1 month (N = 5), which were larger than the untreated 16 month-old *Pde6c$^{cpfl1/cpfl1}$Gnat1$^{IRD2/IRD2}$-Tg(Arc-dVenus)* mice (right); however, visual acuity was similar between these three groups (P = 0.668, ANOVA; left).

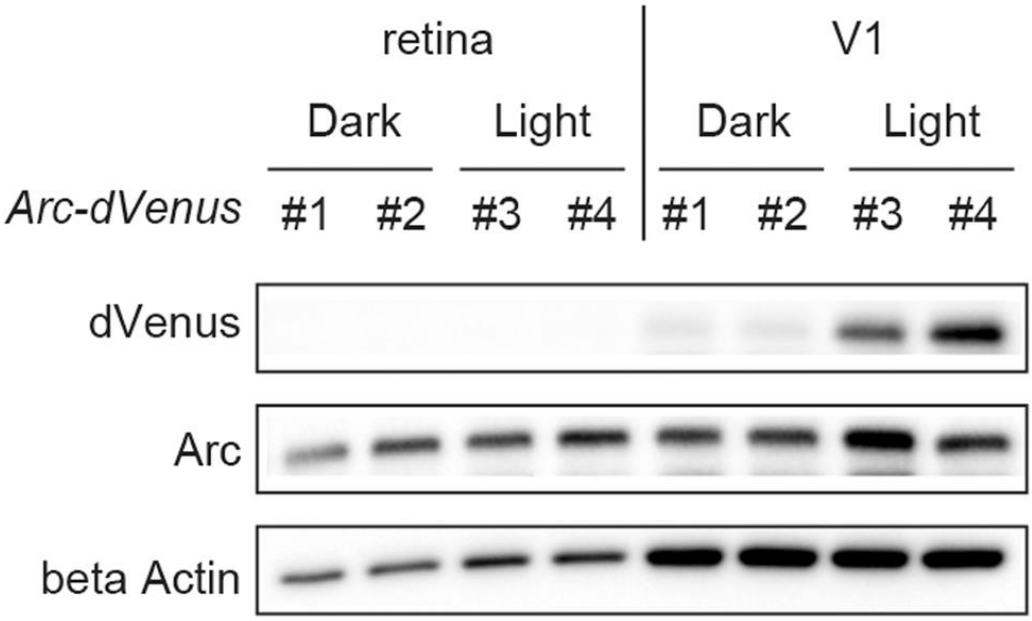

Supplementary Figure S2. High background expression of Arc protein in the dark.

Using *Tg(Arc-dVenus)* mice, we found that the Arc promoter-driven dVenus expression is different under dark (mice #1 and #2) and light (mice #3 and #4) conditions. Similarly, the light-induced upregulation of the endogenous Arc protein was detected in the V1, although the expression of endogenous Arc in the dark was high possibly due to the stabilization of the Arc protein in synapses under synaptically inactive conditions (Mabb et al., 2014).

Mabb AM, *et al.* (2014) Triad3A regulates synaptic strength by ubiquitination of Arc. *Neuron* 82:1299-1316.